

2.75 THz tuning with a triple-DFB laser system at 1550 nm and InGaAs photomixers

Anselm J. Deninger · A. Roggenbuck · S. Schindler · S. Preu

Received: 13 October 2014 / Accepted: 25 November 2014 /

Published online: 10 December 2014

© The Author(s) 2014. This article is published with open access at Springerlink.com

Abstract To date, exploiting the full bandwidth of state-of-the-art InGaAs photomixers for generation and detection of continuous-wave (CW) THz radiation (typ. ~50 GHz to ~3 THz) required complex and costly external-cavity diode lasers with motorized resonator control. Distributed feedback (DFB) lasers, by contrast, are compact and inexpensive, but the tuning range per diode is limited to ~600 GHz at 1.5 μm . In this paper, we show that a combination of three DFB diodes covers the complete frequency range from 0 – 2750 GHz without any gaps. In combination with InGaAs-based photomixers for terahertz generation and detection, the system achieves a dynamic range of > 100 dB at 56 GHz, 64 dB at 1000 GHz, and 26 dB at 2500 GHz. A field-programmable gate array (FPGA)-based lock-in amplifier permits a flexible adjustment of the integration time from 0.5 ms to 600 ms. Employing an optimized “fast scan” mode, a spectrum of ~1200 GHz – the bandwidth of each subset of two lasers – and 40 MHz steps is acquired in less than one minute, still maintaining a reasonable dynamic range. To the best of our knowledge, the bandwidth of 2.75 THz presents a new record for DFB-based CW-terahertz systems.

Keywords Terahertz spectroscopy · Frequency domain · Distributed feedback lasers · InGaAs photomixers · Optoelectronics

1 Introduction

Over the past few years, optoelectronic continuous-wave (CW) terahertz systems operating in the communication wavelength band of 1.5 μm have undergone an impressive performance boost. Emitter and detector photomixers benefit both from the availability of telecom-qualified

A. J. Deninger (✉) · A. Roggenbuck · S. Schindler
TOPTICA Photonics AG, Lochhamer Schlag 19, 82166 Gräfelfing, Germany
e-mail: anselm.deninger@toptica.com

S. Preu
Department of Electrical Engineering and Information Technology, Technische Universität Darmstadt,
Merckstraße 25, 64283 Darmstadt, Germany

components and from established InGaAs/InP processing techniques. On the emitter side, ultrafast p-i-n photodiodes have proven successful in generating respectable terahertz power levels; promising designs include “n-i-pn-i-p” superlattice structures [1–3], waveguide-integrated (WIN) photodiodes [4, 5], and uni-traveling carrier (UTC) diodes [6–8]. Highly sensitive receiver photomixers employ multi-layer stacks of Be-doped LT-InGaAs layers and InAlAs trapping layers [9]. A recent publication by Göbel et al. has demonstrated that a combination of a WIN photodiode emitter and an optimized, coherent receiver achieves a dynamic range beyond 100 dB and a bandwidth of 3.5 THz [10]. These photomixer modules are already commercially available.

Yet on the laser side, challenges have remained. Exploiting the full bandwidth of today’s InGaAs photomixers requires external-cavity diode lasers with motorized resonator control, in other words: complex technology with a price tag in the range of 30,000 EUR per laser. This is generally considered prohibitively high for “real-world” applications. The situation thus resembles that of the early days of GaAs photomixers, when bandwidths beyond 3 THz were demonstrated with “good old” Ti:Sapphire lasers [11, 12] which were intricate in construction and craft sensitive to operate.

Distributed feedback (DFB) lasers present a much more compact and carefree alternative: Similar to a voltage-controlled oscillator, the radiation emitted by a DFB diode depends on well-controlled parameters (chip temperature and driver current) in a reproducible fashion. DFB lasers at 0.8 μm have become the “workhorses” for GaAs photomixers [13–17]: owing to the large thermal tuning coefficient of ~ 25 GHz/K per diode [18], a twin-DFB system at 0.8 μm typically offers a difference frequency tuning range of 0–2000 GHz [19]. At telecom wavelengths, however, conditions are different: Whilst DFB lasers are widely available throughout the telecom band – and even so in highly integrated “butterfly” packages –, their thermal tuning coefficient amounts to no more than ~ 12 GHz/K. A temperature sweep of 50 K (the limit of most temperature controllers) thus translates into a scan range of ~ 600 GHz per laser. This restricts the tuning range of a two-color DFB system at 1.5 μm to 1200 GHz at most.

In this work, we present a system composed of three DFB diodes with carefully selected wavelength offsets. Operating two lasers at a time, we are able to cover difference frequencies from 0 – 2750 GHz without any gaps. We control the frequency of each laser with the help of look-up tables, and achieve an absolute accuracy of better than 1 GHz even without active frequency control. InGaAs photomixers convert the laser beat to terahertz signals, with a peak dynamic range of > 100 dB and still 26 dB at 2500 GHz. To the best of our knowledge, this is the widest bandwidth obtained with a DFB-based terahertz system in the telecom band – and at a laser price that is an order of magnitude below that of an external-cavity system.

2 Wavelength Selection

Let ν_1, ν_2, ν_3 denote the center frequencies of the three laser diodes (i.e. at center temperatures $T_c = 25$ °C), with $\nu_1 < \nu_2 < \nu_3$. The thermal tuning coefficients of the individual diodes are $\frac{d\nu_1}{dT}$, $\frac{d\nu_2}{dT}$ and $\frac{d\nu_3}{dT}$, respectively, and $\pm\Delta T$ is the thermal tuning range around the center temperature. The tuning range of an individual laser diode is then $\nu_i \in [\nu_i - \frac{d\nu_i}{dT}\Delta T; \nu_i + \frac{d\nu_i}{dT}\Delta T] = [\nu_i^{\min}, \nu_i^{\max}]$.

In order to reach zero difference frequency, the frequencies of lasers #1 and #2 have to overlap at the limits of their respective tuning ranges:

$$\nu_1^{\max} = \nu_1 + \frac{d\nu_1}{dT}\Delta T \equiv \nu_2 - \frac{d\nu_2}{dT}\Delta T = \nu_2^{\min}, \quad (1)$$

which determines the choice of the center frequency of laser #2:

$$\nu_2 = \nu_1 + \left(\frac{d\nu_1}{dT} + \frac{d\nu_2}{dT} \right) \Delta T. \tag{2}$$

In order to achieve a continuous spectral coverage without any gaps, the minimum difference frequency of the laser diode pair [#2, #3] has to match the maximum difference frequency of laser diode pair [#1, #2], yielding

$$\nu_2^{\max} - \nu_1^{\min} = \nu_2 - \nu_1 + \left(\frac{d\nu_1}{dT} + \frac{d\nu_2}{dT} \right) \Delta T \equiv \nu_3 - \nu_2 - \left(\frac{d\nu_2}{dT} + \frac{d\nu_3}{dT} \right) \Delta T = \nu_3^{\min} - \nu_2^{\max}. \tag{3}$$

Inserting Eq. (2) in Eq. (3), we find for the center frequency of the third laser

$$\nu_3 = \nu_1 + \left(3 \frac{d\nu_1}{dT} + 4 \frac{d\nu_2}{dT} + \frac{d\nu_3}{dT} \right) \Delta T. \tag{4}$$

The highest difference frequency attainable with combination [#1, #3] is then

$$\Delta\nu_{\max} = \nu_3^{\max} - \nu_1^{\min} = \left(4 \frac{d\nu_1}{dT} + 4 \frac{d\nu_2}{dT} + 2 \frac{d\nu_3}{dT} \right) \Delta T. \tag{5}$$

Inserting typical numbers, $\frac{d\nu_1}{dT} \approx \frac{d\nu_2}{dT} \approx \frac{d\nu_3}{dT} \approx 12$ GHz/K, and $\Delta T=25$ K (corresponding to a working range of the diode temperature controllers of $2\Delta T=50$ K), we obtain for the offsets of the center frequencies $\nu_2 - \nu_1 = 600$ GHz (corresponding to $\Delta\lambda \sim 4.9$ nm), $\nu_3 - \nu_1 = 2400$ GHz (corresponding to $\Delta\lambda \sim 19.5$ nm), and a maximum difference frequency according to Eq. (5) of $\Delta\nu_{\max} = 3000$ GHz. In theory, the maximum difference frequency attainable with a triple-laser combination is thus five times greater than the tuning range of a single DFB laser. Our actual choice of wavelengths was more conservative, since we did not attempt to have the frequencies overlap at the extreme ends of the tuning ranges. We chose diodes with tuning ranges of 1559.5-1564.4 nm (laser #1), 1554.9-1559.9 nm (laser #2) and 1542.2-1547.5 nm (laser #3), as shown in Fig. 1. This combination yields a difference frequency coverage from DC to 2750 GHz.

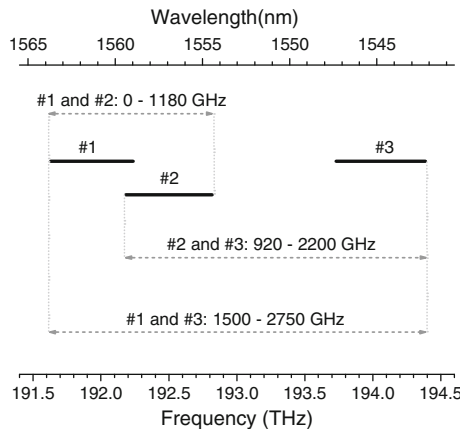


Fig. 1 Tuning range of lasers #1 - #3 (solid lines) and accessible frequencies for the respective two-laser pairs (dotted arrows)

3 System Components

3.1 Lasers

The laser assembly consists of three butterfly-packaged DFB diodes, mounted in compact laser heads (DL DFB BFY, Toptica Photonics). A 50 dB fiber-inline isolator was spliced in the output fiber of each laser diode to protect the diodes from spurious back reflections. We used a fiber-optic 2x2 coupler, made of polarization-maintaining single-mode fibers, to combine the outputs of a chosen pair of diodes.

All lasers were thermally tuned. Calibration data of the wavelength vs. chip temperature were recorded with a Fizeau-type wavelength meter (WS6-IR, HighFinesse), and stored in look-up tables as described in [5]. A field-programmable gate array (FPGA)-based module (“TeraControl”) uses the look-up tables to generate analog voltage signals that drive the set point levels of the respective temperature controllers. The TeraControl also provides a USB interface to an external laptop or PC.

3.2 Photomixers and Terahertz Optics

We utilized InGaAs-based photomixers manufactured by Fraunhofer Heinrich Hertz-Institute Berlin [5, 10]. The photomixers are available as packaged devices with fiber pigtail and integrated silicon lens. The terahertz output power is approx. 48 μ W at 100 GHz, 4 μ W at 500 GHz and 400 nW at 1 THz [20] and the residual beam divergence, according to the manufacturer, is $\sim 12^\circ$ FWHM at 500 GHz. We built a simple setup with two 1” mirrors to collimate the output of the emitter and refocus the beam onto the receiver.

3.3 Data Acquisition

We used lock-in detection to readout the terahertz photocurrent of the receiver. To this end, we chopped the bias voltage of the transmitter ($-1.4 / +0.6$ V, 12 kHz) and demodulated the pre-amplified receiver photocurrent. Spectra were recorded without any delay stage, but rather by scanning the “phase fringes” in small frequency steps (~ 40 MHz), a method detailed in refs. [16, 19].

Our FPGA-based control unit permits an arbitrary choice of the lock-in integration time between 0.5 ms and 600 ms. The time required for the acquisition of a complete spectrum is determined by the number of frequency steps and the integration time per step. A scan across 1200 GHz, at a step size of 40 MHz and an integration time of 300 ms, takes approx. 3 hrs, including some “overhead” time for data transfer. Faster scanning is possible if compromises with respect to the dynamic range are acceptable; however, we found that the USB interface between the FPGA and the PC initially presented an ultimate “bottleneck” with a bandwidth limit of ~ 15 Hz. This means that no matter how short the integration time, the acquisition time for the same scan would never fall below 35 minutes. We therefore developed and implemented a “fast scan” mode, where sets of 1000 data points are temporarily stored in the FPGA, and transferred *en bloc* to the PC. This algorithm reduces the USB traffic significantly: A scan with an integration time of 3 ms and otherwise identical settings (1200 GHz range, 40 MHz step size, i.e. a spectrum of 30000 data points) is now recorded in 90 s, i.e. 23 times faster. At an integration time of 0.5 ms, the acquisition time reduces to 15 s, beating the previous limit by a factor of 140.

4 Results and Discussion

A spectrum of the dynamic range of the terahertz power, from frequencies between 50 GHz and 2.75 THz, is shown in Fig. 2. The (power) dynamic range DR in dB is calculated via

$$DR = 20 \times \log(I_{\text{Signal}}/I_{\text{Noise}}), \quad (6)$$

where I_{Signal} denotes the signal photocurrent and I_{Noise} is the noise current of the receiver, measured with zero transmitter bias. The spectra in Fig. 2 present combined data of all laser combinations. The upper curve was recorded with a lock-in integration time of 300 ms per frequency step, the lower one shows a fast scan with 3 ms per step. The shorter integration time increases the noise level of the lock-in signal ($I_{\text{noise}} \propto [\text{integration time}]^{-1/2}$) and consequently, a factor of 100 in the integration time reduces the dynamic range by 20 dB.

With 300 ms/step (lock-in bandwidth, ENBW ~ 1.7 Hz), we measure a peak dynamic range of 101.5 dB at 56 GHz. At higher frequencies, we obtain 64 dB at 1000 GHz, 42 dB at 2000 GHz and 26 dB at 2500 GHz. These values confirm the excellent performance of the InGaAs photomixers as reported in [10]; the fact that our values are slightly lower than those reported by Göbel et al. is attributed to the use of 1" (rather than 2") mirrors in our setup: the mirror diameter may have been too small to collimate the terahertz beam in particular at low frequencies, where the beam divergence increases.

The dips in the spectrum of Fig. 2 are absorption signatures of water vapor. The vertical lines on the bottom of the graph represent literature values from the HITRAN database. Comparing the frequencies of the measured line centers to the HITRAN values, we find a deviation of (-0.4 ± 0.7) GHz for the spectrum with 300 ms integration time (mean value \pm standard deviation of all water lines discernible between 557 GHz and 2686 GHz). This underlines the accuracy of the wavelength calibration scheme and demonstrates that precise frequency control is feasible even without closed-loop regulation.

For the fast scan with 3 ms integration time, the water lines appear red-shifted by (1.5 ± 0.8) GHz (mean value \pm standard deviation of all water lines discernible between 557 GHz and 2464 GHz). This frequency shift, more readily seen in the close-up of Fig. 3, is attributed to thermal inertia of the DFB diodes: the temperatures are scanned so rapidly that the temperature

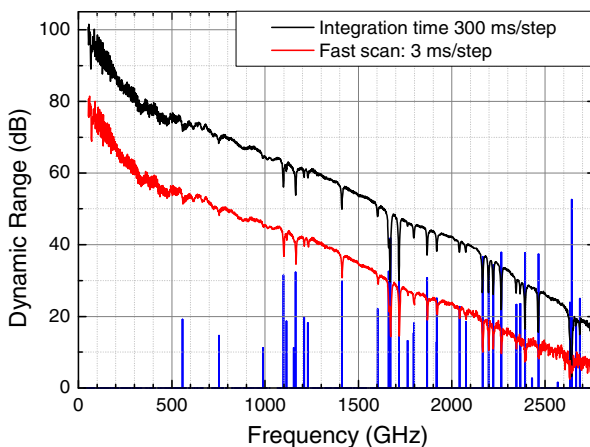


Fig. 2 Dynamic range of the terahertz power from 50 GHz to 2750 GHz. The vertical lines on the bottom indicate the absorption frequencies of water vapor [21]; the height of the lines corresponds to the line strength on a logarithmic scale

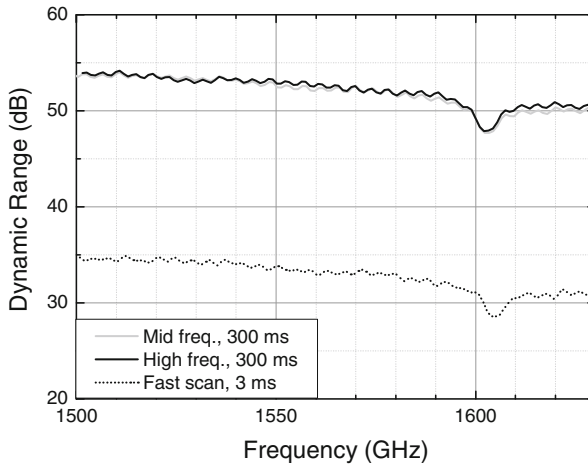


Fig. 3 Close-up of the overlap region of laser combinations [#2, #3] (grey) and [#1, #3] (black). Both the signal level and the frequency calibration match for the two laser pairs. The dotted trace shows the corresponding “fast scan” spectrum, where the water line at 1603 GHz appears red-shifted by ~ 2 GHz

control loop cannot follow exactly. For fast scans acquired in the same direction, i.e. as long as “up” and “down” scans are not mixed, this offset can readily be corrected by data post-processing software. In other words, since the frequency offsets are reproducible under identical measurement conditions, the spectral resolution and repeatability are not limited by the aforementioned absolute accuracy.

The systems supports a minimum integration time of 0.5 ms. Such short integration times, however, result in fairly large frequency offsets of ~ 10 GHz for a step size of 40 MHz. For high-resolution measurements, however, shorter integration times can be used without compromising the frequency accuracy: A step size of, e.g., 6 MHz and an integration time of 0.5 ms yield a similar accuracy as the aforementioned scan with 40 MHz step size and 3 ms integration time, since the overall tuning speed is approximately constant (12–13 GHz/s, corresponding to a thermal scanning speed of ~ 0.5 K/s/laser).

The curves in the top of Fig. 3 illustrate the overlap between the “mid-frequency” [lasers #2, #3] and “high-frequency” [lasers #1, #3] regimes and illustrate that not only the frequencies, but also the dynamic range levels measured with both combinations are in excellent agreement. The ripples visible in the signal have a period of ~ 4.2 GHz, which implies that they originate from multiple reflections within the Silicon lenses of the packaged photomixer modules [22].

As shown in Fig. 4, frequency steps of 1 MHz still produce a smooth signal. Using the aforementioned values of dv/dT , this minute step width indicates that our electronics actually controls the laser temperatures with a resolution on the order of 40 μ K. We note that 1 MHz is already close to the approximate beat signal linewidth: We measured the linewidth of a single 1.5 μ m DFB diode with the help of a delayed self-heterodyne beat technique [23] and obtained a value of 650 kHz on a time scale of 100 μ s, resulting in a beat signal linewidth of $\sqrt{2} \cdot 650$ kHz = 920 kHz. The high frequency resolution, attainable throughout the tuning range of our lasers, is another significant advantage compared to motorized external-cavity systems, which have a typical resolution of ~ 10 pm or ~ 1 GHz.

The dynamic range of our optoelectronic spectrometer is already close to that of state-of-the-art, frequency-extended RF systems. Crowe et al. [24] reported on a frequency-extended

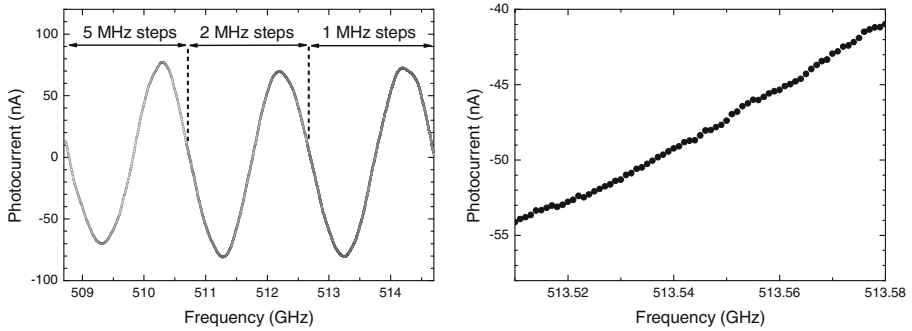


Fig. 4 left: Terahertz photocurrent, at step sizes of 5 MHz, 2 MHz and 1 MHz. Right: close-up of a section of the scan, showing individual 1 MHz steps

vector network analyzer (VNA) in the WR1.0 band, centered around 900 GHz with a dynamic range of 70 dB at an ENBW of 10 Hz. For the same measurement bandwidth (corresponding to a lock-in time constant of 50 ms), the photomixing system provides a dynamic range of 58 dB at 900 GHz, i.e. only 12 dB lower, not even taking transmission losses into account. A major disadvantage of frequency-extended VNAs is their limited tuning range. A single waveguide band offers only a bandwidth of less than 20% of the center frequency. If a larger frequency range needs to be accessed, the complete extender setup has to be exchanged. It may also require a realignment of the terahertz setup, adjusted to the new extender. Covering the range of, e.g., 100 GHz – 1000 GHz would require about 7 sets of extenders, and about 10 sets would be necessary for the range from 100 GHz – 2700 GHz. By contrast, each subset of two DFB laser diodes in our photomixing system offers a tuning range of more than 1 THz already. The complete spectrum from 50 GHz – 2750 GHz is compiled from three sections recorded with the respective subsets of two lasers. Exchanging the lasers does not affect the terahertz alignment and is fairly simple. An interesting future perspective is the option of driving all lasers simultaneously, a concept recently demonstrated with GaAs photomixers [25]. The latter technique, however, necessitates a phase delay to separate the different beat signals again, so the gain in measurement speed is traded off against a higher complexity of the optical setup and less terahertz power at each individual frequency.

Similar to the VNA, the photomixer setup allows for accessing both amplitude and phase. The (much) coarser resolution and broader linewidth of ~ 1 MHz of the free running system does not play any role for the majority of applications. If required, a sub-Hz-level linewidth could be achieved by locking to a compact CW frequency comb as shown in refs. [26, 27]. Photomixing systems may therefore be an option for replacing RF circuitry in future VNAs [28], offering much larger frequency ranges without switching between bands, and less system complexity at just slightly lower dynamic range.

5 Conclusion

InGaAs-based photomixers for CW-terahertz generation and detection have attained remarkable performance levels. Yet, the comparatively small tuning range of telecom-band DFB diodes – approx. 600 GHz per laser – has hindered their use in wideband spectroscopy. We show that a triple-DFB laser setup with carefully selected wavelength offsets produces a range of difference frequencies that is up to five times greater than the tuning range of a single laser.

The setup described here covers difference frequencies from 0 GHz to 2750 GHz without any gaps and thus achieves a bandwidth that used to be accessible with external-cavity diode lasers only, yet at a fraction of the cost. Employing a combination of a waveguide-integrated photodiode as terahertz emitter, and a Be:InGaAs/InAlAs multilayer structure as coherent receiver, our setup achieves a dynamic range of 101.5 dB at 56 GHz and 64 dB at 1.0 THz, at a lock-in integration time of 300 ms per frequency step. A “fast scan” mode reduces the measurement time for each subset of two lasers from 35 min to 90 s for an integration time of 3 ms, by minimizing the data traffic across the system’s USB interface. The fast scan causes a frequency red-shift of 1.5 GHz, due to thermal inertia of the DFB diodes. The spectral resolution of ~ 1 MHz is not affected by the offset. In the future, we plan to implement a real-time measurement of the actual DFB laser temperatures, which will help reduce thermal hysteresis effects.

Acknowledgements SP acknowledges funding by the Hessian “LOEWE-Sensors Towards Terahertz” program. AD, AR and StS acknowledge funding by the German Federal Ministry for Economic Affairs and Energy (BMW, “ZIM” project KF 2806201PR0) for the development of the “Fast Scan” routine.

Open Access This article is distributed under the terms of the Creative Commons Attribution License which permits any use, distribution, and reproduction in any medium, provided the original author(s) and the source are credited.

References

1. G.H. Döhler, F. Renner, O. Klar, M. Eckardt, A. Schwanhäußer, S. Malzer, D. Driscoll, M. Hanson, A.C. Gossard, G. Loata, T. Löffler, H. Roskos, “THz-photomixer based on quasi-ballistic transport,” *Semicond. Sci. Technol.*, vol. 20, no. 7, pp. 178-190, 2005.
2. S. Preu, F.H. Renner, S. Malzer, G.H. Döhler, L.J. Wang, M. Hanson, A.C. Gossard, T.L.J. Wilkinson, E.R. Brown, “Efficient terahertz emission from ballistic transport enhanced n-i-p-n-i-p superlattice photomixers,” *Appl. Phys. Lett.*, vol. 90, no. 21, pp., 212115-212117, 2007.
3. S. Preu, G.H. Döhler, S. Malzer, L.J. Wang, and A.C. Gossard, “Tunable, continuous-wave terahertz photomixer sources and applications,” *J. Appl. Phys.*, vol. 109, pp. 61301-61356, 2011.
4. H.-G. Bach, A. Beling, G.G. Mekonnen, R. Kunkel, D. Schmidt, W. Ebert, A. Seeger, M. Stollberg, W. Schlaak, “InP-based waveguide-integrated photodetector with 100-GHz bandwidth,” *IEEE J. Quantum Electron.*, vol. 10, no. 4, pp. 668-672, 2004.
5. D. Stanze, A. Deninger, A. Roggenbuck, S. Schindler, M. Schlak, B. Sartorius, “Compact cw terahertz spectrometer pumped at 1.5 μm wavelength,” *J. Infrared Milli. Terahz. Waves*, vol. 32, no. 2, pp. 225-232, 2011.
6. T. Ishibashi, N. Shimizu, S. Kodama, H. Ito, T. Nagatsuma, T. Furuta, “Uni-traveling-carrier photodiodes,” in: “Ultrafast Electronics and Optoelectronics,” M. Nuss and J. Bowers, eds., Vol. 13 of *OSA Trends in Optics and Photonics Series*, paper UC3, 1997.
7. H. Ito, T. Nagatsuma, A. Hirata, T. Minotani, A. Sasaki, Y. Hirota, T. Ishibashi, “High-power photonic millimeter-wave generation at 100 GHz using matching-circuit-integrated uni-travelling-carrier photodiodes,” *Proc. Inst. Elect. Eng. Optoelectron.*, vol. 150, pp. 138-142, 2003.
8. E. Rouvalis, C.C. Renaud, D.G. Moodie, M.J. Robertson, A.J. Seeds, “Traveling-wave uni-traveling carrier photodiodes for continuous wave THz generation,” *Opt. Express*, vol. 18, pp. 11105-11110, 2010.
9. B. Sartorius, M. Schlak, D. Stanze, H. Roehle, H. Künzel, D. Schmidt, H.-G. Bach, R. Kunkel, M. Schell, “Continuous wave terahertz systems exploiting 1.5 μm telecom technologies,” *Opt. Express*, vol. 17, pp. 15001-15007, 2009.
10. T. Göbel, D. Stanze, B. Globisch, R.J.B. Dietz, H. Roehle, M. Schell, “Telecom technology based continuous wave terahertz photomixing system with 105 dB signal-to-noise ratio and 3.5 terahertz bandwidth,” *Opt. Lett.*, vol. 38, no. 20, pp. 4197-4199, 2013.

11. E.R. Brown, K.A. McIntosh, K.B. Nichols, C.L. Dennis, “Photomixing up to 3.8 THz in low-temperature-grown GaAs,” *Appl. Phys. Lett.*, vol. 66, no. 3, pp. 285–287, 1995.
12. K.A. McIntosh, E.R. Brown, K.B. Nichols, O.B. McMahon, W.F. di Natale, T.M. Lyszczarz, “Terahertz photomixing with diode lasers in low-temperature-grown GaAs,” *Appl. Phys. Lett.*, vol. 67, no. 26, pp. 3844–3846, 1995.
13. I.S. Gregory, M.J. Evans, H. Page, S. Malik, I. Farrer, H.E. Beere, “Analysis of photomixer receivers for continuous-wave terahertz radiation,” *Appl. Phys. Lett.*, vol. 91, no. 15, pp. 154103–154105, 2007.
14. J.R. Demers, R.T. Logan Jr., E.R. Brown, “An optically integrated coherent frequency-domain THz spectrometer with signal-to-noise ratio up to 80 dB,” *Microwave Photonics Tech. Digest*, Victoria, Canada, pp. 92–95, 2007.
15. A.J. Deninger, T. Göbel, D. Schönherr, T. Kinder, A. Roggenbuck, M. Köberle, F. Lison, T. Müller-Wirts, P. Meissner, “Precisely tunable continuous-wave terahertz source with interferometric frequency control,” *Rev. Sci. Instr.*, vol. 79, no. 4, pp. 44702–44707, 2008.
16. A. Roggenbuck, H. Schmitz, A. Deninger, I. Cámara Mayorga, J. Hemberger, R. Güsten, M. Grüninger, “Coherent broadband continuous-wave terahertz spectroscopy on solid-state samples,” *New J. Phys.*, vol. 12, pp. 43017–43029, 2010.
17. M. Scheller, M. Stecher, M. Gerhard, M. Koch, “Hybrid continuous wave terahertz spectroscopy,” *Opt. Express*, vol. 18, pp. 15887–15892, 2010.
18. S. Kraft, A. Deninger, C. Trüch, J. Fortágh, F. Lison, C. Zimmermann, “Rubidium spectroscopy at 778–780 nm with a distributed feedback laser diode,” *Laser Phys. Lett.*, vol. 2, no. 2, pp. 71–76, 2005.
19. A. Deninger, “State-of-the-art in terahertz continuous wave photomixer systems,” in: “Handbook of Terahertz Technology,” D. Saeedkia, ed., *Woodhead Publishing Series in Electronic and Optical Materials*, 2013.
20. D. Stanze, “Komponenten und Systeme zur Dauerstrich-THz-Spektroskopie auf Basis optischer Telekommunikationstechnologien,” PhD thesis, University of Bochum (Germany), 2014.
21. HITRAN database, see <http://www.cfa.harvard.edu/hitran/>
22. M. Langenbach, A. Roggenbuck, I. Cámara Mayorga, A. Deninger, K. Thirunavukkuarasu, J. Hemberger, M. Grüninger, “Group delay in THz spectroscopy with ultra-wideband log-spiral antennae,” *J. Infrared Milli. Terahz. Waves*, vol. 35, no. 11, pp. 918–931, 2014.
23. T. Okoshi, K. Kikuchi, A. Nakayama, “Novel method for high resolution measurement of laser output spectrum,” *Electron. Lett.*, vol. 16, pp. 630–631, 1980.
24. T.W. Crowe, B. Foley, S. Durant, K. Hui, Y. Duan, J.L. Hesler, “VNA frequency extenders to 1.1 THz,” *Proc. IRMMW-THz*, Houston, TX, 2011.
25. A. Roggenbuck, K. Thirunavukkuarasu, M. Langenbach, E. Vidal, H. Schmitz, J. Hemberger, M. Grüninger, “High-precision phase determination in a continuous-wave terahertz spectrometer by heterodyning of three lasers,” *Proc. IRMMW-THz*, Tucson, AZ, 2014.
26. A.R. Criado, C. de Dios, G.H. Döhler, S. Preu, S. Malzer, S. Bauerschmidt, H. Lu, A.C. Gossard, P. Acedo, “Ultra-narrow linewidth CW sub-THz generation using GS based OFCG and n-i-pn-i-p superlattice photomixers,” *Electron. Lett.*, vol. 48, pp. 1425–1426, 2012.
27. S. Preußler, N. Wenzel, R.-P. Braun, N. Owschimikow, C. Vogel, A. Deninger, A. Zadok, U. Woggon, T. Schneider, “Generation of ultra-narrow, stable and tunable millimeter- and terahertz- waves with very low phase noise,” *Opt. Express*, vol. 21, pp. 23950–23962, 2013.
28. A.R. Criado, C. de Dios, P. Acedo, H.-L. Hartnagel, “New concepts for a photonic vector network analyzer based on THz heterodyne phase-coherent techniques,” *Proc. 7th European Microwave Integrated Circuits Conference (EuMIC)*, Amsterdam, pp. 540–543, 2012.